A numerical approach to modelling the effect of a static pressure field on the frequency response of a clamped thin circular plate

Kyle Saltmarsh[1], Ali Karrech[2], David Matthews[1,3] and Jie Pan[1]

[1]School of Mechanical & Chemical Engineering, The University of Western Australia, Perth, Australia
[2]School of Civil, Environmental and Mining Engineering, The University of Western Australia, Perth, Australia
[3]Underwater Sensors Group, Defence Science and Technology Group, HMAS Stirling, Australia

ABSTRACT

A detailed understanding of the vibrational properties of submerged objects such as submarines is essential in order to minimise sound emission and optimise sonar performance. Complications arise when hollow structures are submerged in water producing loading on one side. Not only does the water dampen the resonances of the structure but also the increase in depth produces mechanical strain within the structure that changes the resonant frequencies. In previous work, the effect of hydrostatic pressure loading on one side of a rigidly clamped plate was investigated. The modal coupling between the water tank and the vibrating plate hindered the ability to observe the experimental dependence of the plate's frequency response on the applied hydrostatic pressure. In this paper some results are presented on the effect of static pressure loading produced by air on the plate, removing the complications introduced by fluid loading and modal coupling. The aim of this work is to accurately measure these effects experimentally and identify similarities and any interesting discrepancies with the numerical models used for prediction. The finite element package ABAQUS was used to model the frequency response of the plate subjected to a static pressure field produced by a finite air cavity.

1. INTRODUCTION

A detailed understanding of the vibrational properties of submerged objects such as submarines is essential in order to minimize sound emission and optimise sonar performance. The effect of hydrostatic pressure on the modal frequencies of submerged hollow structures is a complex problem. Modelling such effects using conventional finite element methods and boundary element methods is difficult. The accuracy of these models is heavily reliant on user intuition and non-systematic methods. Significant discrepancies between results and predictions were found during the frequency and mode shape analysis of a torpedo model submerged in water (Pan and Matthews, 2011). Efforts were then made to experimentally characterise the effects of hydrostatic pressure on the frequency response of a thin rigidly clamped circular plate (Saltmarsh et al, 2015). This investigation yielded interesting yet ambiguous results due to the presence of acoustic-structural coupling. The presence of tank and coupled plate-tank modes made it difficult to identify the plate mode dependence on the hydrostatic pressure. Observations drawn from the frequency response of the plate-tank rig yielded both increasing and decreasing modes, with varying dependencies. Experimental or coupled theoretical-experimental work in this area is scarce but there are many applications where such effects are very important and need to be understood.

In this work, some results are presented on the effects of a static pressure field produced by an air cavity on the frequency response of the thin rigidly clamped circular plate. Some preliminary experimental results are presented and compared with the finite element model. Significant focus has been applied to the construction and verification of the finite element model, with a detailed description of the analysis methods used.

2. EXPERIMENTAL SETUP

Figure 1 shows a schematic diagram of the plate test rig used for experimental analysis. A thin steel plate is clamped rigidly between two steel flanges with a much greater mass disparity to suppress the effects of structural coupling between the plate and the rig. By using such a configuration, it was possible to avoid some of the environmental complications encountered in the hydrostatic measurements mentioned above. A steel backing plate is bolted to one of the flanges to produce an enclosed acoustic air cavity on one surface of the plate. The backing plate possesses a valve to allow the adjustable pressurization of the air cavity. Thin 1 mm rubber gaskets were

placed between the plate, flange and backing plate to ensure that the pressurized air cavity is effectively sealed. A positive pressure pump was used to increase the static gauge pressure from 0 Pascal to 10 Kilopascal in 0.5 Kilopascal increments. An impact hammer was used to excite the plate. This method of excitation was selected over a mechanical shaker to eliminate the effects of mass loading. A single accelerometer (PCB 352C67) of mass 5 g was used to measure the acceleration of the plate due to the mechanical excitation. Both the strike and accelerometer locations were selected as irrational ratios of the plate's radius to ensure no specific modes were being suppressed or explicitly excited. Figure 1 shows the experimental setup for the test rig.

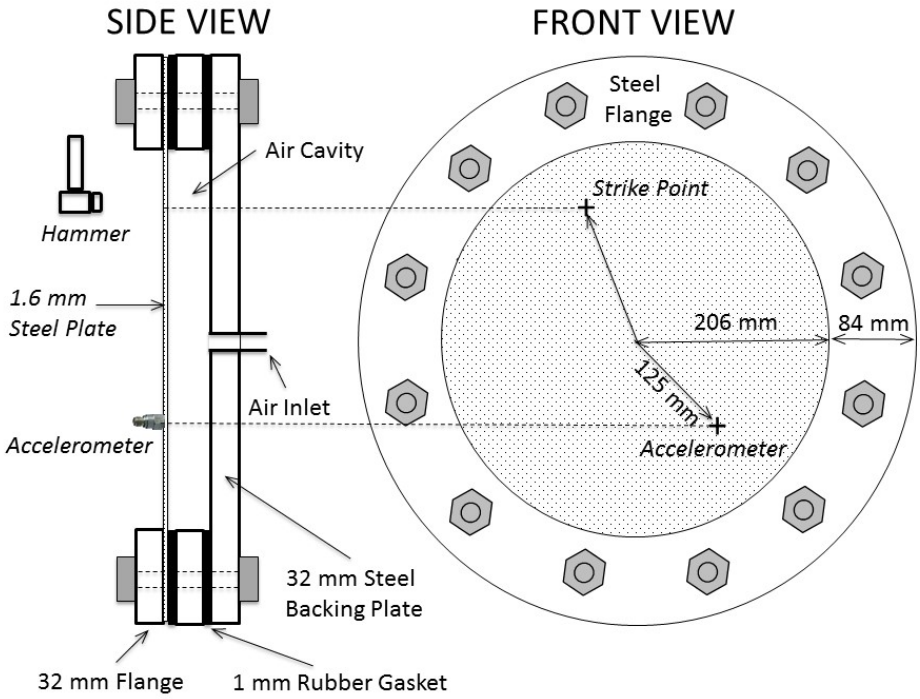

Figure 1: Schematic of test rig detailing components

The software package PULSE (Brüel & Kjær, 2015) was used to measure the accelerometer output and impact force. The frequency response functions of the plate were then generated through computing the ratio of the acceleration to impact force. This quantity is defined as the transfer accelerance. This system was limited to a 1 Hz resolution.

3. FINITE ELEMENT MODEL

The finite element model was constructed using the software package ABAQUS (Dassault Systèmes, 2014). The model includes the plate, rubber gaskets, flanges, bolts, backing plate and the air cavity as depicted in figure 1.

3.1 Geometric And Material Properties

The geometric and material properties for the entirety of the test rig are detailed in table 1. These were the values that were used in the finite element model for theoretical comparison to experimental results. The density, Young's modulus, Bulk modulus, Poisson's ratio, outside diameter, inner diameter and thickness are given by the symbols ρ, E, K, v, OD, ID and t, respectively.

Table 1: Experimental test rig properties

Geometry	Material	ρ *(Kg/m^3)*	E (GPA)	K (GPA)	*v*	OD *(mm)*	ID *(mm)*	t (mm)
Circular Plate	Mild Steel	7800	210	175	0.3	580	-	1.6
Gasket seal	Rubber	1000	1E-3	6.25 E-3	0.47	580	412	2
Flange	Mild Steel	7800	210	175	0.3	580	412	32
Backing Plate	Mild Steel	7800	210	175	0.3	580	-	32
Acoustic Cavity	Air	1.225	-	1.01 E-4	-	412	-	32
Bolts	Mild Steel	7800	210	175	0.3	-	-	-

3.2 Element Type

Due to the disparity between the plate's thickness and planar dimensions, the shell planar elements S4R were used for modelling. The element type S4R is a reduced integrated, general-purpose, finite-membrane-strain shell element. The element's membrane response is treated with an assumed strain formulation that gives accurate solutions to in-plane bending problems, is not sensitive to element distortion, and avoids parasitic locking. Reduced integration is suitable due to minimal deflection amplitude with hourglass control activated to avoid spurious deformation within the mesh.

The flanges, bolts, rubber gaskets and backing plate were all modelled using the solid element C3D8R. The element type C3D8R is a reduced integrated, hourglass controlled general purpose 3-D stress solid element. The coupled mass-stiffness matrix for the flanges and backing plate effectively result in minimal stresses and strains in these geometries.

The air cavity was modelled utilising the acoustic element type AC3D8. This element type allows fluid-structural coupling between the air cavity and the test rig. The acoustic element type can only sustain pressure differentials due to acoustic loading and hence does not deform due to the plate's vibration. Energy balance contributions are present as the acoustic energy is distributed between the plate geometry and the air cavity.

3.3 Procedural Steps

The analysis comprised three separate procedures. Steps may fall into either the general analysis or the linear perturbation procedural types. The classification of the analysis is determined by the linearity of the response. Simulations utilising linear and non-linear analysis were applied to determine the appropriate classification when considering the induced stress and deflection of the plate. The deflections at the centre of the plate as a function of pressure are shown in figure 2 for the linear solution, non-linear solution and the theoretical solution for a loaded clamped plate. The discrepancy between the theoretical and linear finite element solution is due to the nature of the clamped boundary condition assumed by each model. The theoretical solution assumes a perfectly clamped edge whilst the finite element model has assumed a finite value of stiffness for the boundary condition that will result in larger displacements which is depicted by the plot. Due to the curvature of the non-linear solution it was determined that the application of the pressure field to the surface of the plate over the range from 0 to 10 kPa yields a non-linear response.

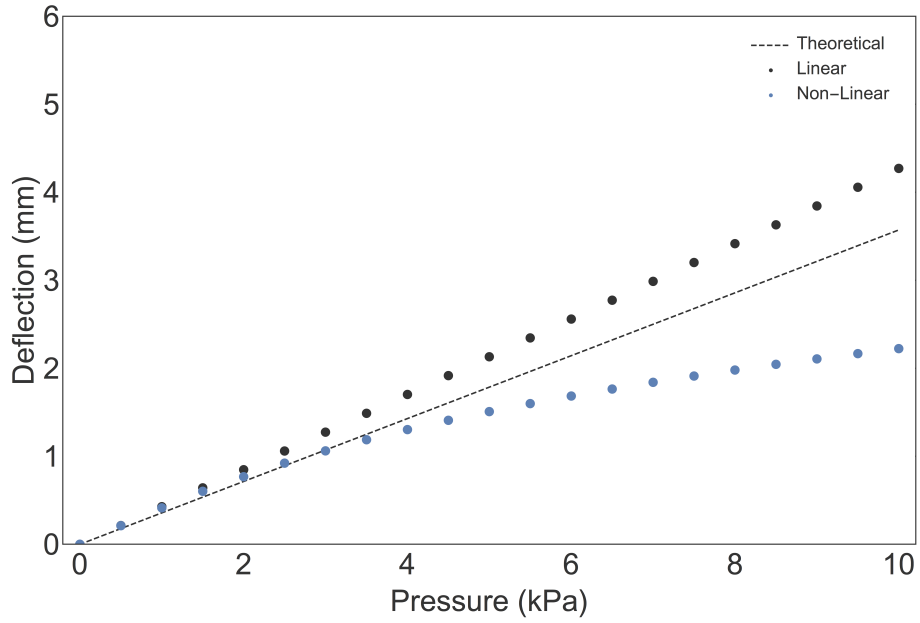

Figure 2: Comparisons for the center plate deflections over the pressure range 0 to 10 kPa

The selected analysis step was then chosen to be a *Static, General* step. The resulting stresses and strains produced are transferred to the base state for the following step. The analysis is time independent and hence the load is applied incrementally, with the stiffness and mass matrices updated accordingly. The details for this step are outlined in table 2.

Table 2: Static, General step details

Parameter	Value
Procedure Name	Static
Procedure Type	General
Non-Linear Geometry	Yes
Automatic Stabilisation	Yes
Energy Fraction	0.0002
Adaptive stabilisation	Yes
Max Ratio to Strain Energy	0.05

The succeeding *Frequency* step is an Eigenmode extraction step to solve for the resonant frequencies and corresponding mode shapes of the system. This step is a linear perturbation step that yields the natural vibration properties of the system not due to excitation. The eigenvalue problem for the natural frequencies of an undamped finite element model is given by equation 1.

$$\left(-\omega^2 M^{MN} + K^{MN}\right)\phi^N = 0 \tag{1}$$

Where M^{MN} is the mass matrix (symmetric and positive definite), K^{MN} is the stiffness matrix, ϕ^N is eigenvector (the mode of vibration) and *M* and *N* are degrees of freedom. The details for this step are outlined in table 3.

Table 3: Frequency step details

Parameter	Value
Procedure Name	Frequency
Procedure Type	Linear Perturbation
Eigensolver	Lanczos
Acoustic-Structural Coupling	Yes
Eigenvector Normalisation	By Mass
Max Frequency	1000 Hz

The final procedure is the *Modal Dynamics* step. This is a transient linear dynamics procedure that solves the system through modal super positioning. The Eigenmodes used in this analysis are those of which were solved in the *Frequency* step. An impulse load is applied to the plate at the experimental striking location depicted in figure 1. The excitation is given as a function of time and that its magnitude varies linearly with each increment. When the model is projected onto the Eigenmodes the following set of equations are obtained at time t.

$$\ddot{q}_\beta + C_{\beta\alpha}\dot{q}_\alpha + \omega_\beta^2 q_\beta = \left(f_t\right)_\beta = f_{t-\Delta t} + \frac{\Delta f}{\Delta t}\Delta t \tag{2}$$

Where the α and β indices span the eigenspace, $C_{\beta\alpha}$ is the projected viscous damping matrix, q_β is the response amplitude of the mode β, $\omega_\beta = \sqrt{k_\beta/m_\beta}$ is the natural frequency of the undamped mode β, $(f_t)_\beta$ is the magnitude of the loading projected onto this mode and Δf is the change in frequency over the time increment Δt. The solution to the uncoupled equations is obtained as a particular integral for the loading and a solution to the homogenous equation. These solutions can be combined to give equation 3.

$$\begin{Bmatrix} q_{t+\Delta t} \\ \dot{q}_{t+\Delta t} \end{Bmatrix} = \begin{bmatrix} a_{11} & a_{12} \\ a_{21} & a_{22} \end{bmatrix} \begin{Bmatrix} q_t \\ \dot{q}_t \end{Bmatrix} + \begin{bmatrix} b_{11} & b_{12} \\ b_{21} & b_{22} \end{bmatrix} \begin{Bmatrix} f_t \\ f_{t+\Delta t} \end{Bmatrix} \tag{3}$$

Where a_{ij} and b_{ij} are constants as the loading varies linearly over the time increment. The dynamic response of the plate inclusive of stresses, strains and accelerations are then calculated for a specified time period. The sampling frequency and time period of the analysis were selected to be 2 Kilohertz and 1 second respectively, to produce a Nyquist frequency of 1000 Hz with a 1Hz resolution akin to the experiment. The details of this step are outlined in table 4.

Table 4: Modal dynamics step details

Parameter	Value
Procedure Name	Modal Dynamics
Procedure Type	Linear Perturbation
Time Period	1 s
Time Increment	0.0005 s
Critical Damping Fraction	0.002
Load Type	Impulse
Load Time	0.005 s

3.4 Interactions

Interaction pairs have been created between the plate, flanges, backing plate, bolts and air cavity. The interactions between the bolts, flanges and backing plate were modelled as surface-to-surface contact with the friction coefficient of steel on steel as 0.05. The rubber gaskets are connected to both the plate and the flanges using the tie constraint that ensures constant contact. The air cavity is connected to a single surface of the plate using the tie constraint. The air mesh is selected as the slave surface so that the nodes will conform to match the deformation of the plate nodes.

3.5 Boundary Conditions And Loads

Fixed boundary conditions were applied to the interface between the rubber gaskets and steel flanges, bolts and the interface between the plate and the bolts. Application of the fixed boundary to the rubber gasket rather than the plate introduces damping at the boundary conditions that is what is observed experimentally. Fixing the bolts supresses the vibration of the virtually rigid steel flanges and backing plate.

The impulse load applied in the Modal Dynamics step was designed as a ramp load over a time period of 0.005 seconds. The integral of the impulse load yields a total applied force of 1 N to simplify finding the response.

4. RESULTS

The purpose of this finite element modelling is to characterize the effects of a static pressure field on the frequency response of plate structures, in particular a circular plate with clamped edges. Comparisons are made between the experimental results and finite element model firstly for ambient conditions with no pressure field to ensure good agreement is found and to hence validate the model. Comparisons are then made for the phenomenon observed within the frequency response of the plate with the application of the static pressure field.

4.1 Plate Response at Ambient Pressure

Figure 2 shows the transfer accelerance functions for the plate rig for both experimental and finite element methods at ambient pressure conditions. Good agreement is found between the two methods up to the 8^{th} resonant frequency in both peak location and response function shape.

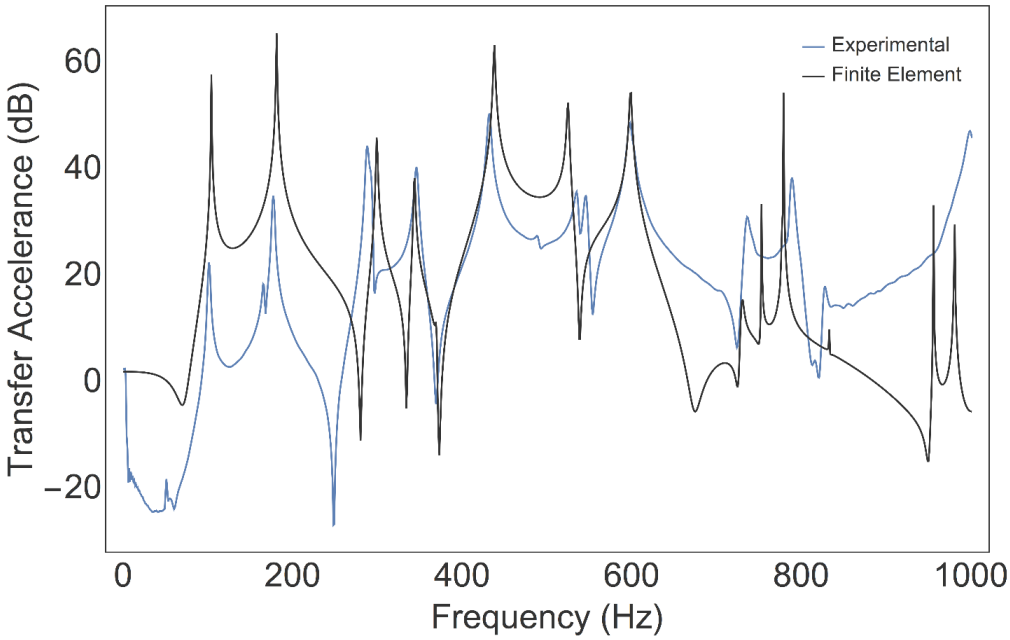

Figure 3: Transfer accelerance from experimental and finite element results at ambient pressure

Table 5 details the comparisons of the resonant frequencies for the first 6 peaks. The mode number (m,n) is also given where m and n represent the number of diametral modes and number of circular modes respectively. Generalised, m represents the mode number whilst n represents the harmonic number. The discrepancies between the experimental results and finite element model across these peaks ranged from 0.58 to 3.82 %, with an average of 2.15 %. It can be seen that the finite element model cannot accurately model the experimental response function for higher order modes as its accuracy declines heavily beyond 800 Hertz. With the exception of the model splitting observed in the experimental peaks numbered 2 and 6, the characteristics of the response function shape are also modeled accurately. This can be noticed when observing the regions between peaks as well as the trend in the peak amplitudes themselves. This level of agreement validates the ability of the finite element model to predict the response of the test rig for the pressure simulations.

Table 5: Experimental and finite element resonant frequency comparison

Peak	Mode	Experimental (Hz)	Numerical (Hz)	Difference (%)
1	(0,1)	101	104	2.97
2	(1,1)	177, 165	181	2.26
3	(2,1)	288	299	3.82
4	(0,2)	346	344	0.58
5	(3,1)	432	438	1.39
6	(1,2)	535, 546	525	1.87

4.2 Plate Response With Applied Pressure

The application of the static pressure field to one surface of the vibrating plate was found to produce significant changes to the frequency response characteristics for both the experimental and finite element methods. Figures 3 and figure 4 depict the waterfall plots for the experimental and finite element transfer accelerance functions respectively, ranging from 0 Pascal to 10 Kilopascal in 0.5 Kilopascal increments.

Through inspection the resonant frequencies of the response functions corresponding to the modes of the vibrating plate are observed to increase. This is as expected as the application of the pressure produces tension within the plate (Leissa, 1969). Unlike the results from the hydrostatic pressure (Saltmarsh et al, 2015), the results obtained here allow the direct comparison with theoretical prediction as each mode can be confidently identified. Table 6 summarises the observed resonant frequency movements with pressure.

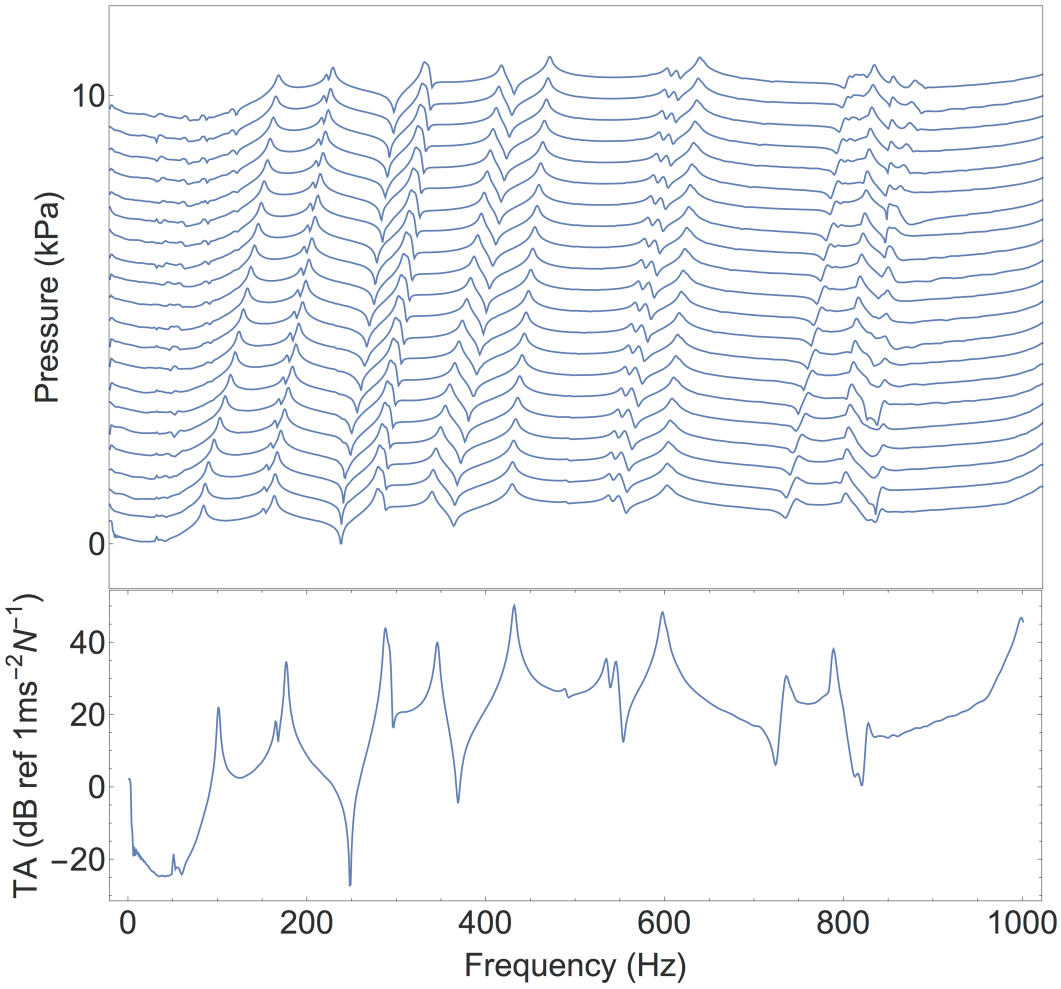

Figure 4: Waterfall plot depicting the variation in the transfer accelerance for the experimental measurements ranging from 0 kPa to 10 kPa in 0.5 kPa increments

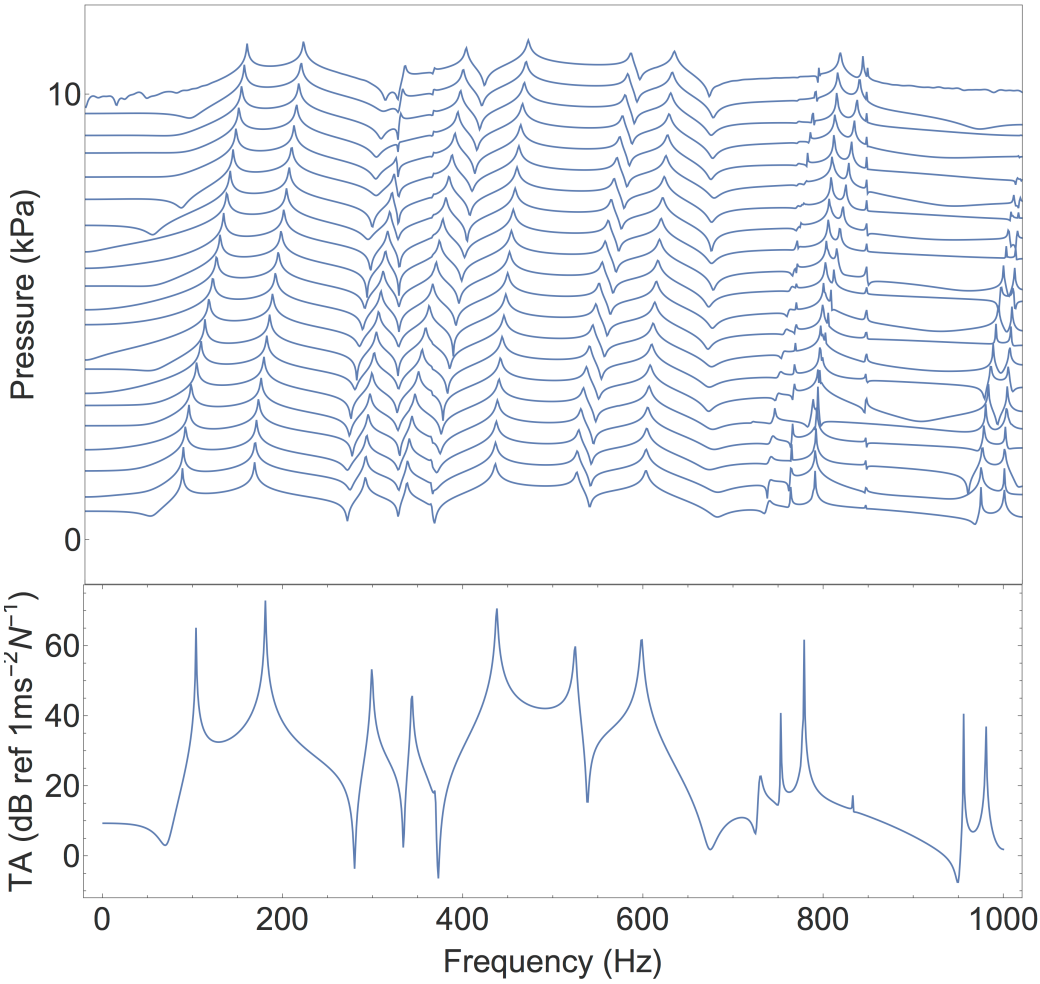

Figure 5: Waterfall plot depicting the variation in the transfer accelerance for the finite element simulation ranging from 0 kPa to 10 kPa in 0.5 kPa increments

Table 6: Increases in experimental and finite element resonant frequency comparison over an air pressure increase of 10 kPa

Peak	Mode	Experimental Shift (%)	Numerical Shift (%)
1	(0,1)	80.20	66.35
2	(1,1)	41.21, 35.59	28.73
3	(2,1)	17.36	14.38
4	(0,2)	21.39	18.31
5	(3,1)	9.26	7.99
6	(1,2)	11.78, 11.36	10.86

The comparison between the experimental and finite element results shows good agreement for modes 3 to 6. The discrepancies found between the resonant frequency shifts for modes 1 and 2 are fairly considerable, however the trend between the degree of movement of each mode is identical. Both the experimental and finite element results highlight that there is a clear dependence between the resonant frequency movement and the associated mode number. It is observed that there is a decreasing dependency with increasing mode number m, which is evident when comparing the shifts harmonic modes (0,2) and (1,2) with fundamental modes (2,1) and (3,1).

5. CONCLUSIONS

It has been shown both experimentally and theoretically that the application of a static pressure field produced by an air cavity to one surface of a vibrating plate increases the resonant frequencies of the structure. Substantial increases were observed for relatively small pressures, however it is noted that the geometry and stiffness of the disc ultimately determine the subsequent stresses and strains produced in the plate. These preliminary results however show the criticality of these effects on the frequency response of plate structures, and validate their theoretical counterparts produced with finite element software ABQUS. Further investigation into the effects on the mode shapes, the consequent sound radiated pressure and the strain produced in the plate will yield an in-depth experimental and theoretical characterization of the effect of pressure fields on the frequency response of vibrating structures.

REFERENCES

Brüel & Kjær, 2015, *PULSE Version 42*, software program, Brüel & Kjær, Nærum, Denmark.

Dassault Systèmes, 2014, *ABAQUS 6.14-1*, software program, Dassault Systèmes, Vélizy-Villacoublay, France.

Leissa, A. W. (1969), Vibration of Plates, Scientific and Technical Information Division, National Aeronautics and Space Administration, Washington.

Liu, W, et al (2010), *'Measurement of sound radiation from torpedo-shaped structure subject to an axial excitation'*, Proceedings of 20th International Congress on Acoustics. Available from: ICA digital library. [August 2010].

Pan, J and Matthews, D (2011) 'Analysis of underwater vibration of a torpedo-shaped structure subjected to axial excitation', Proceedings of Acoustics 2011, the 2011 Conference of the Australian Acoustical Society. Available from: AAS digital library. [November 2011].

Matthews D, et al (2014), *'A detailed experimental modal analysis of a clamped circular plate'*, Proceedings of InterNoise 2014, the 2014 Conference of the Australian Acoustical Society. Available from: AAS digital library. [November 2014].

Saltmarsh K, (2014), *'The effects of sound radiation environment on structural vibration'*, Honours thesis, School of Mechanical and Civil Engineering, The University of Western Australia.

Saltmarsh K, et al (2015), *'Effect of water pressure on the frequency response of a thin rigidly clamped plate'*, in Y Zhou, A.D Lucey, Y Liu and L Huang (eds), FSSIC 2015: Fluid-Structure-Sound Interaction and Control; "Proceedings of the 3rd Symposium on FSSIC", Curtin University, Perth, Western Australia, pp. 89-94.